Synthesis of Water Soluble Sulfonated Polyaniline and Determination of Crystal Structure

Sambhu Bhadra,[1] Nam Hoon Kim,[2] Joong Hee Lee[1,2]

[1]*Department of Polymer and Nano Engineering, BIN Fusion Research Team, Chonbuk National University, Duckjin-dong 1Ga 664-14, Jeonju, Jeonbuk 561-756, South Korea*
[2]*Department of Hydrogen and Fuel Cell Engineering, Chonbuk National University, Duckjin-dong 1Ga 664-14, Jeonju, Jeonbuk 561-756, South Korea*

ABSTRACT: A polyaniline (PANI) was synthesized by the oxidative polymerization using ammonium persulfate as an oxidizing agent. The PANI was then stirred with excess fuming sulfuric acid at room temperature for 6 h to obtain water soluble sulfonated polyaniline (SPANI). The degree of sulfonation was found to be 93–94% from the Fourier transform infrared (FTIR) and elemental analysis. The solubility of the SPANI in water was 1.25 g/L at room temperature and appeared as a green color solution. Conductivity of the PANI was decreased after sulfonation. A proliferation of hydrophilic nature of the PANI after sulfonation was observed from the water contact angle measurement. From the UV analysis, it was revealed that the energies required for the π–π^* and bipolaron/polaron transitions are less and the intensity of these transitions are lower in SPANI compared to those of PANI. A detailed study on the crystal structures of PANI and SPANI were accomplished from the powder X-ray diffraction analysis. The SPANI exhibited a more ordered structure having a higher degree of crystallinity and crystallite sizes with an increased unit cell volume compared to the PANI. After sulfonation the morphology of PANI was transformed from a rod-like shape to a flat-plate shape. © 2010 Wiley Periodicals, Inc. J Appl Polym Sci 117: 2025–2035, 2010

Key words: conducting polymers; crystal structures; FTIR; X-ray

INTRODUCTION

Polyaniline (PANI) is one of the most attractive polymers in the intrinsically conducting polymer group because of its ease of synthesis, substantial thermal stability, tunable properties, and numerous application possibilities.[1–7] However, the main problem associated with PANI for its effective utilization is inherent in its insolubility in most of the available organic solvents. Nevertheless, the solubility of PANI can be enhanced through doping with a suitable dopant or by modifying the starting monomer.[3,6] While dopant significantly increases the conductivity of PANI, the increase in the solubility is not significant.[3] When the aniline containing different aromatic substitutions is polymerized, the resulting substituted PANI exhibits a greater solubility in organic solvents, yet the conductivity decreases to a large extent compared to unsubstituted PANI. It is assumed that, when substituted aniline is polymerized, the planarity of the aromatic rings in the resulting substituted PANI is lost due to steric hindrance exerted by substituents and, as a result, conductivity decreases.[6] The research idea for this study is based on the incorporation of an aromatic substitution in the polymer (PANI) rather than in the monomer (aniline) to retain its planer structure and hence conductivity.

If a polymer is soluble in water, then it can be processed in a water medium without using any solvent. Processing of a water soluble polymer is a less expensive and a more environmentally friendly method. PANI has the ability to retard corrosion.[8,9] Hence, it can be added in a paint to retard the corrosion on different metal surfaces. However, paints are mostly water based. Therefore, for the utilization of PANI as an anticorrosive agent in water based paints, it must be soluble in water. Water soluble PANI can be prepared through the incorporation of suitable aromatic substituents, such as phenolic, carboxylic, sulfonic acid groups in PANI. The introduction of a sulfonic acid group at the aromatic ring of PANI is the simplest and cost effective method (one step, solvent and catalyst are not required) to obtain water soluble PANI with considerable conductivity.

The sulfonic acid group is expected to solubilize PANI in a water medium. Since the sulfonic acid group will be incorporated in PANI (rather than in aniline), it is expected that the planarity of the aromatic rings will be retained, and, hence, there may not be a significant loss of conductivity due to the incorporation of an aromatic substitution. Additionally, the sulfonic acid group in sulfonated PANI (SPANI) acts as a doping agent and forms a stable six-membered self-doping ring structure with imine or amine nitrogen. As a result, the conductivity of SPANI remains stable over a wide range of pH levels ($0 \leq pH \leq 14$).[10,11]

The crystal structure affects the melting point, solubility, stability, and crystal morphology of an organic compound.[12] Although PANI is a semi-crystalline polymer, in-depth studies on its crystal structure are scanty.[7,13] The crystal structure of a compound is generally derived from its single-crystal diffraction. The process involves the development of a single crystal of the material, its optical analysis, determination of crystal system and unit cell dimension, measurement of crystal density, calculation of unit cell, recording of hkl and determination of space group.[14–17] The process is wearisome, and sometimes it is challenging to grow a single crystal from the crystalline material.[13] A relatively tranquil method for the determination of the crystal structure is the powder X-ray analysis, though the method has several limitations.[14] The computer simulation of a crystal structure using different software packages is becoming an increasingly attractive method.[12] Fullprof is a widely used software package for this purpose, although it is generally utilized to analyze fully crystalline inorganic materials.[18–20] The reports on the crystal structure analysis of semi-crystalline organic polymers such as PANI by using different software packages are very rare, though the subject has great potential.[7]

This research deals with the synthesis of PANI by the chemical oxidative polymerization of aniline, the sulfonation of synthesized PANI to produce water soluble sulfonated PANI (SPANI). An in-depth investigation of the crystal structure of PANI and SPANI was also carried out through a powder X-ray diffraction analysis using FullProf and FOX v. 1.7. OSVN softwares.

EXPERIMENTAL

Materials

The materials used in this study include aniline (Kanto Chemical Co. Inc., Japan), ammonium persulfate (APS) (Sigma Aldrich, Germany), methanol (Samchun Pure Chemicals Co. Ltd., Korea), hydrochloric acid, and sulfuric acid (Duksan Pure Chemi-

cals Co., Ltd., Korea). All these chemicals are of a GR grade. Aniline was distilled before use while the other chemicals were used as received.

Synthesis of polyaniline

Aniline 9.3 mL (0.1 M) and 2 mL (0.05 M) of conc. HCl (50 mol % with respect to aniline) were placed into a beaker containing 100 mL distilled water and were stirred for 5 min with a magnetic stirrer to obtain a homogeneous mixture. APS of 22.8 g (0.1 M) (equimolar amount with respect to aniline) was then dissolved in 10 mL of water. This aqueous solution of APS was added in drops to the reaction beaker containing aniline in water. The polymerization reaction was carried out for 6 h at room temperature (25 $\pm$ 5°C) with constant stirring. The molar ratios of monomer (aniline) to oxidant (APS) of 1 : 1 and monomer to dopant (HCl) of 1 : 0.5 were fixed because an earlier study revealed that these ratios result in good yield and conductivity of the resultant polymer.[3] After 6 h of polymerization, the reaction was stopped through the addition of 50 mL methanol. A deep green PANI was precipitated, which was filtered, thoroughly washed with distilled water to remove unreacted chemicals, and then dried in a vacuum oven at 60°C for 48 h. Finally, the dried PANI powder was rewashed using methanol and dried in a vacuum oven at 60°C for 48 h.

Sulfonation of polyaniline

The PANI thus synthesized was placed into a beaker with excess fuming H_2SO_4, and the mixture was stirred with a magnetic stirrer for 6 h at room temperature (25 $\pm$ 5°C). The mixture was then slowly poured into ice water (75 : 25), and a green precipitate was then filtered and washed several times with ice water until a constant pH was obtained (to remove excess acid). The residue was then dried in a vacuum oven at 60°C for 48 h. Finally, the dried powder was rewashed using methanol and dried in a vacuum oven at 60°C for 48 h. This sulfonated PANI is designated as SPANI.

Characterization

The electrical conductivity was measured under laboratory conditions by the four-point probe method using a programmable DC voltage detector, a 2182A NANOVOLTAMETER (Keithley), and a 6220 precision current source (Keithley). Sample powder was compacted into a disk pellet with a diameter of 12.6 mm and a thickness of about 0.25 mm by applying a pressure of 10 tons. All data presented is the average value of the measurements from at least five samples.

The water contact angle was measured under laboratory conditions using a Phoenix-300 from Surface Electrooptics, Korea. The powder was compacted into a disk pellet under a pressure of 10 tons, and the contact angle of water on this pellet was measured.

The Fourier transform infrared (FTIR) spectra were recorded on a NICOLET 6700 FTIR (Thermoscientific). Samples were dispersed in KBr powder and compressed into pellets. OMINIC software was used for the base line correction and calculation of the peak area.

To obtain the degree of sulfonation in SPANI, the elemental analysis was carried out using an Automatic Elemental Analyzer, specifically the Flash EA 1112 Series from Thermo Fisher Scientific.

The thermogravimetric analysis (TGA) was accomplished using a TGA, specifically Q50 from TA Instruments. The experiment was carried out under a nitrogen atmosphere over the temperature range of 35–900°C and at the heating rate of 20°C/min.

The UV-visible spectra were acquired at ambient temperature using a UVS-2100 SCINCO spectrophotometer. Stock solutions were prepared by dissolving each sample (0.5 g/L) in tetrahydrofuran (THF) and then filtering them through a 1.0 μm filter unit.

The X-ray diffraction study was performed using a D/MAX 2500V/PC from the Rigaku Corporation, Japan, using a copper target (Cu Kα), forming an X-ray of wave length of 1.5418 Å. The data was recorded from $2\theta = 5–50°$, since beyond 50° there was no peak.

The scanning electron microscopic (SEM) image was observed using a SEM, the JSM 6400 from Jeol, Japan. Sample powder was spread onto carbon coated copper SEM grids. Samples were coated with gold-palladium before observation.

RESULTS AND DISCUSSION

Conductivity, solubility, and hydrophilicity

In a previous study, it was found that when aniline containing different aromatic substitutions was polymerized, the resulting substituted PANI showed a higher solubility, but with a substantial abatement in conductivity (from 10^{-4} to 10^{-7} S/cm).[6] The main objective of this research was to produce water soluble substituted PANI without significant decrease in conductivity. This was achieved through the sulfonation of PANI. The conductivity of PANI and SPANI are 0.073 and 0.031 S/cm, respectively. The PANI has three basic structures, namely: (I) a fully oxidized pernigraniline base (PNB), where all repeat units have a quinoid structure (Q), (II) a fully reduced leucoemeraldine base (LEB), where all repeat units have a benzenoid structure (B), and (III) a half oxidized emeraldine base (EB), where the Q to B ratio is 1 [Fig. 1(a)]. After doping of the emeral-
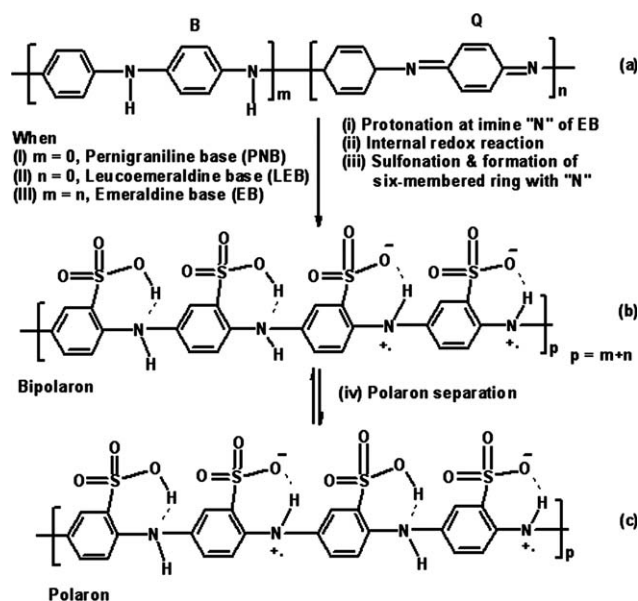

Figure 1 (a) Different structures of PANI based on oxidation levels: (I) fully oxidized pernigraniline base (PNB), (II) fully reduced leucoemeraldine base (LEB) and (III) half oxidized emeraldine base (EB). (b) Bipolaron formation after protonation of EB, sulfonation of PANI and formation of stable six-membered self-doped ring structure. (c) Bipolaron to polaron transition.

dine base (EB), it first forms bipolaron [Fig. 1(b)] and then polaron [Fig. 1(c)]. This polaron is conducting in nature. The LEB and PNB are relatively insulating in nature even after doping.[3,4] The PANI and SPANI are significantly conducting in nature, which implies that these PANI samples contain high concentrations of an EB form. The conductivity of PANI is reduced to some extent after sulfonation. The decrease of conductivity after sulfonation may be due to the negative resonance (−R) effect of the sulfonic acid group. The sulfonic acid group withdraws electrons (-R effect) from the benzene ring, thereby decreasing the electron density at the polymer backbone.[21] However, the sulfonic acid group in sulfonated PANI (SPANI) forms a stable six-membered self-doped ring structure as presented in Figure 1(b–c). As a result, the conductivity of SPANI remains stable over a wide range of pH levels ($0 \leq pH \leq 14$).[10,11] Additionally, after sulfonation PANI becomes water soluble. This is very momentous from the application point of view, especially for the utilization of PANI as an anticorrosive agent in water based paint. The solubility of the SPANI is 1.25 g/L in water at room temperature, whereas the PANI is almost insoluble in water. An enhancement of hydrophilic nature of the PANI after sulfonation was also noticed from the water contact angle measurement. The water contact angle for PANI is 61.8°, which is reduced significantly to 23.1° after sulfonation of PANI. The abatement in water contact angle
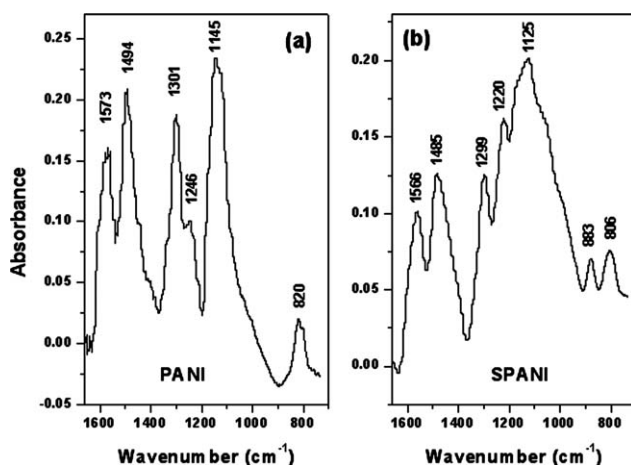
Figure 2 FTIR spectra of (a) PANI and (b) SPANI (samples were dispersed in KBr powder and compressed into pellets before characterization).

for the SPANI implies a proliferation in water wettability or hydrophilicity due to the sulfonation of aromatic rings.[22]

Fournier transform infrared spectra

Figure 2 demonstrates the FTIR spectra of PANI and SPANI. The PANI exhibits six major absorption peaks [Fig. 2(a)], while SPANI displays seven major absorption peaks [Fig. 2(b)] within the same wave number region (700–1700 cm^{-1}). The IR absorption peaks at 1573 and 1494 cm^{-1} for PANI correspond to the quinoid (Q) and benzenoid (B) ring stretching deformations respectively.[4,5,23,24] The band at 1301 cm^{-1} for PANI is assigned for the π electron delocalization induced in the polymer through protonation or C—N—C stretching vibration.[23,24] The band at 1246 cm^{-1} is ascribed to the characteristic of the C—N$^+$ stretching vibration in the polaron structure.[5] The absorption band at 1145 cm^{-1} is due to the vibration mode of the —NH$^+$= in the protonated emeraldine base.[23–25] The band at 820 cm^{-1} is for the C—H out of plane deformation of 1,4-disubstituted benzene ring.[26] All these six absorption bands at 1573, 1494, 1301, 1246, 1145, and 820 cm^{-1} for PANI are red shifted at 1566, 1485, 1299, 1220, 1125, and 806 cm^{-1}, respectively in the SPANI spectrum. The red shift of all these bands in SPANI compared to PANI may be due to the extra protonation[5,26] because the sulfonic acid group acts as a dopant and SPANI forms a self-doped six-membered stable ring structure [Fig. 1(c)].[10,11] Additionally, for SPANI the peak at 1125 cm^{-1} broadens and an extra peak appeared at 883 cm^{-1}. The band for the aromatic C—S stretching appears at ~1100 cm^{-1}.[10] Therefore, this broadening of the band at 1125 cm^{-1} is due to the merging of two bands, namely —NH$^+$= vibration and C—S stretching in SPANI. Compared to the

PANI, the new absorption peak at 883 cm^{-1} in the SPANI is due to the introduction of the SO$_3$H group at the benzene ring of SPANI and assigned for the stretching vibration of S—O.[10] From the ratio of peak area at 883 and 806 cm^{-1}, the degree of sulfonation in SPANI was calculated and found to be 94%. From the elemental analysis of SPANI, the S/N molar ratio was found to be 0.93. Therefore, the degree of sulfonation in SPANI is 93–94%.

Thermogravimetric analysis

The TGA plots of PANI and SPANI are presented in Figure 3. There are four steps of weight loss occurred during the heating of both the polymers under a nitrogen atmosphere. The first step of weight loss that occurred within 50–150°C is due to the loss of moisture. The second step of weight loss is observed in between 150 and 400°C. This step of weight loss is for the loss of dopant HCl and sulfonic acid group in SPANI. The third step of weight loss is found over the temperature range of 400–700°C, which is due to the thermal decomposition of PANI into a number of chemical forms. The fourth step of weight loss at around 700–900°C, which is for the final carbonization of intermediate chemicals.[4,5,23,24,27] The onset and peak temperature of decomposition for the dopant and sulfonic acid group is found to be higher for SPANI compared to that of PANI (second step of weight loss). The higher thermal stability of the sulfonic acid group of SPANI is due to its higher size and molecular weight compared to that of HCl in PANI. The onset and peak temperature of decomposition for the main polymer backbone of PANI and SPANI (third step of weight loss) are almost similar, indicating that the thermal stability after sulfonation of PANI remains unchanged. The ratio of dopant to polymer weight loss is much higher in the SPANI than that of PANI,
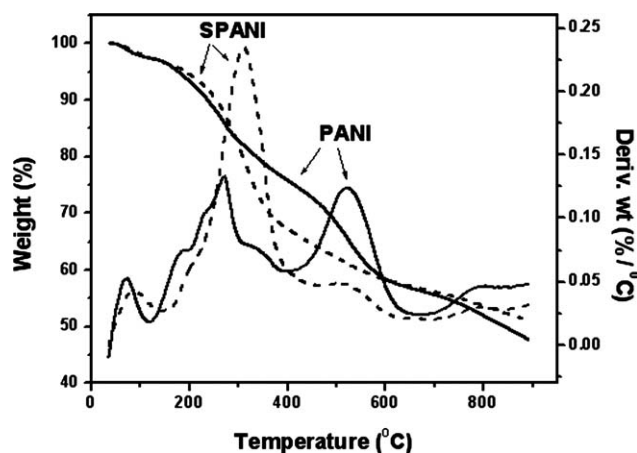

Figure 3 TGA plots of PANI and SPANI (the experiment was carried out under a nitrogen atmosphere at the heating rate of 20°C/min).
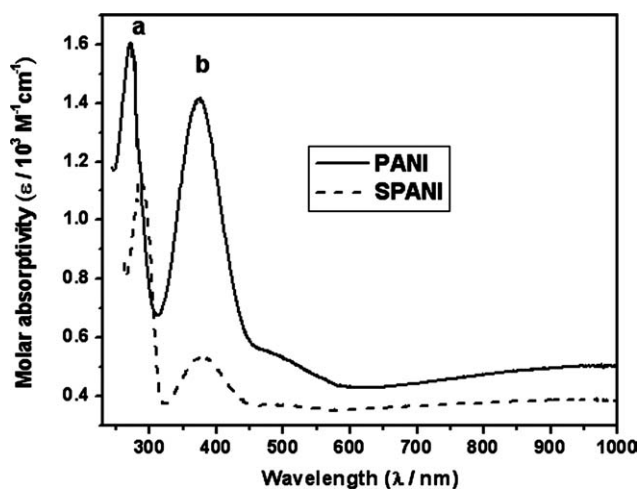
Figure 4 UV spectra of PANI and SPANI (stock solutions were prepared by dissolving each sample (0.5 g/L) in tetrahydrofuran (THF) and then filtering them through a 1.0 μm filter unit).

indicating the extra protonation that occurs after sulfonation. This result is in agreement with the red shift of the absorption peaks in the FTIR spectrum for SPANI. Initially, with the increase in the degree of doping in PANI, the conductivity is expected to enhance via the formation of increasingly more polarons. This is due to the amplification of charge carriers' concentration and their mobility. While at very high doping levels the conductivity is again expected to decrease due to the formation of more bipolarons.[3,4,23,24] The decrease in conductivity after sulfonation may also be due to the formation of more bipolarons through extra protonation.

Ultraviolet-visible spectra

Figure 4 shows the UV spectra of PANI and SPANI. The UV spectra of PANI and SPANI exhibits two characteristic absorption bands; the first band appears over 250–310 nm (band a), and the second band appears within 310–450 nm (band "b"). The first absorption band (a) is attributed to the π–π* transition and the second absorption band (b) is due to the bipolaron/polaron transition that occurs in doped PANI [Fig. 1(b–c)].[23,24] The band energies for different absorption bands were calculated from the following equation,

$$\Delta E = \frac{hc}{\lambda_{\max}} \quad (1)$$

$h = 6.625 \times 10^{-34}$ Js, $c = 3 \times 10^8$ m/s.

Here, ΔE is the band energy, h is the Plank's constant, c is the velocity of light, and $\lambda_{\max}$ is the wave length of maximum absorption.

The wave length of maximum absorption ($\lambda_{\max}$), the calculated band energy (ΔE), and the maximum molar absorptivity ($\varepsilon_{\max}$) of PANI and SPANI for the π–π* (band "a") transition and the bipolaron/polaron (band "b") transition are presented in Table I. The sulfonation of PANI causes an increase in $\lambda_{\max}$ (bathochromisom) for both bands "a" and "b". The band energies of both the bands decrease after sulfonation of PANI. These results indicate that the π–π* and bipolaron/polaron transitions become easier after sulfonation. This may be due to the extra protonation and formation of the self-doped six-membered stable ring structure by the sulfonic acid group and hence the increase in stability of the conjugated system. As both the π–π* and bipolaron/polaron transitions require less energy for SPANI, its conductivity is expected to be higher compared to PANI.[24,27] However, experimentally the conductivity of SPANI is found to be lower than that of PANI. This may be due to the decrease in electron density at the polymer backbone of SPANI because of the −R effect of the sulfonic acid group and could also be due to the formation of more bipolarons through extra protonation, as discussed earlier. The $\varepsilon_{\max}$ for both the transitions are found to decrease (hypochromic shift) after sulfonation of PANI. These decrease in the $\varepsilon_{\max}$ for the π–π* and bipolaron/polaron transitions indicates that the intensity of these transitions are diminished in SPANI leading to an inferior conductivity compared to that of PANI. Thus, the UV result is consistent with the conductivity, FTIR and TGA results.

Powder X-ray crystal structure determination

Analysis of powder X-ray diffraction data

The XY (2*Theta vs. Intensity) data obtained from this experiment was plotted with the WINPLOTR program, and the angular position of the peaks was obtained with the same program.[28] The dimension of the unit cell, hkl values, and the space groups of all these polymers were determined by running the DICVOL program in the FullProf software package.

TABLE I
Wave Length of the Maximum Absorption ($\lambda_{\max}$), Band Energy (ΔE) and the Maximum Molar Absorptivity ($\varepsilon_{\max}$) of PANI and SPANI for π–π* (band "a") and Bipolaron/Polaron (band "b") Transitions

Parameters	PANI	SPANI
$\lambda_{\max}$ for π–π* transition (nm)	271	286
$\lambda_{\max}$ for bipolaron/polaron transition (nm)	374	379
ΔE for π–π* transition (eV)	4.58	4.34
ΔE for bipolaron/polaron transition (eV)	3.32	3.28
$\varepsilon_{\max}$ for π–π* transition ($\times 10^3 \, M^{-1} \, \mathrm{cm}^{-1}$)	1.6	1.1
$\varepsilon_{\max}$ for bipolaron/polaron transition ($\times 10^3 \, M^{-1} \, \mathrm{cm}^{-1}$)	1.4	0.5

Refinement was then carried out through the routine profile matching of FullProf.[29–32] The arrangement of the polymer chains in the unit cell was resolved using the FOX v. 1.7. OSVN software after substituting the values of the unit cell dimensions and the space group obtained from the DICVOL program. The orientation was optimized, and the configuration was randomized. The XY (2θ vs. Intensity) was also plotted using Origin 6.1. Smoothing of the curves was carried out by adjacent averaging methods considering of 5 points. A straight line was then subtracted to obtain $Y = 0$. Finally, a Gaussian fit for multiple peaks was carried out to obtain areas of different peaks as well as their full width at half maxima. The degree of crystallinity (%) was calculated from the ratio of crystalline peak area to total peak area. The d-spacing (D) corresponding to different crystalline peaks was determined by the Debye-Scherrer (powder) method using Bragg's relation[33,34]

$$n\lambda = 2D \sin \theta. \qquad (2)$$

Here, n is an integer, λ is the wavelength of the X-ray, which is 1.54 Å for the Cu target, and θ is the angle between the incident and reflected rays.

The crystallite size (T) of different crystalline peaks were determined from the Scherrer relation[35]

$$T = \frac{K\lambda}{B \cos \theta}. \qquad (3)$$

Here, K is the shape factor for the average crystallite ($\sim$0.9), and B is the full width at half maxima of the crystalline peak in radians.

Result of X-ray powder analysis

A semi-crystalline polymer such as PANI has two different regions: crystalline and amorphous. The crystalline region is called crystallite, where the polymer chains are orderly arranged. The region where the chains are not orderly arranged is known as the amorphous region. The X-ray diffraction plots of polyaniline (PANI) and sulfonated polyaniline (SPANI) are presented in Figure 5. Different crystalline peaks are found for both the polymers. The crystal planes (d_{hkl}) corresponding to the main crystalline peaks are shown in the corresponding figures and in Table II. It is interesting to note that after sulfonation of PANI there is a change in the X-ray diffraction plot. Six crystalline peaks are observed for the PANI at different angles of diffraction [Fig. 5(a)]. Among these crystalline peaks, two peaks are sharper with a much higher intensity. These two peaks are located at $2\theta = 20.4°$ corresponding to the d_{-211} crystal plane, and at $2\theta = 25.4°$ corresponding to the d_{211} crystal plane. The sharpness (width) of
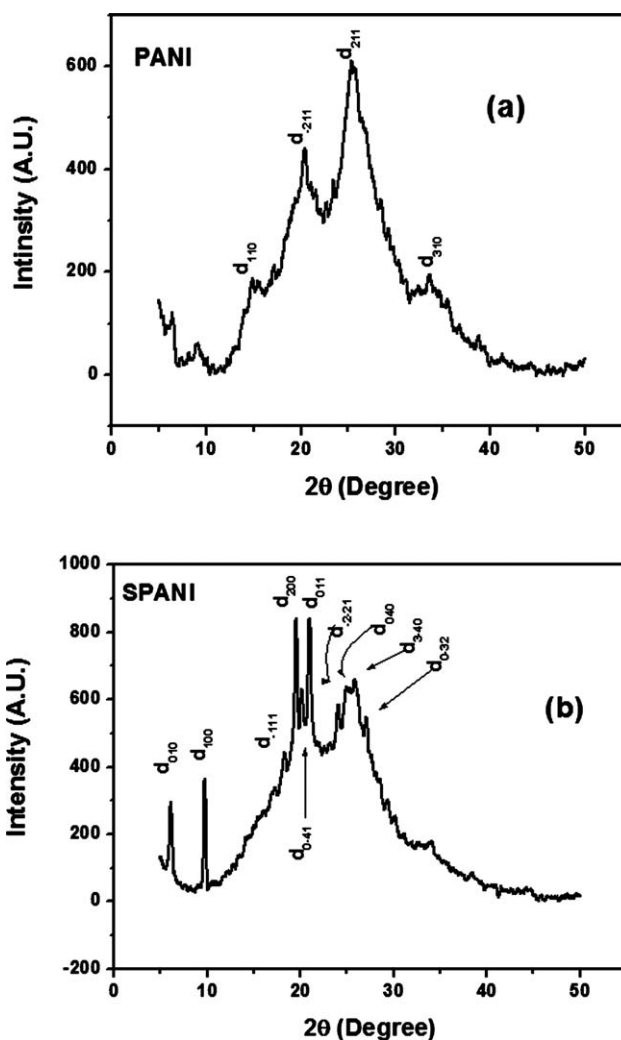

Figure 5 X-ray powder diffraction plot of (a) PANI and (b) SPANI (XY data was plotted using Origin 6.1, smoothen by adjacent averaging methods considering 5 points, a straight line was subtracted to obtain $Y = 0$).

the peaks represents the degree of orientation of the polymer chains in that particular crystal plain and the intensity (peak height) represents the population of crystallite in that plane.[7] The X-ray diffraction pattern of PANI indicates that the majority of PANI chains are orderly arranged on the d_{211} crystal plane. However, SPANI [Fig. 5(b)] manifests a higher number of crystalline peaks (10) and most of them are very sharp with a high intensity compared to that of PANI. Several crystalline peaks indicate that the crystallites of SPANI are oriented in several directions or several crystal planes (more heterogeneity of orientation), while sharper peaks proves that polymer chains are more ordered in the crystalline region and a higher intensity implies more crystalline regions leading to a higher crystallinity compared to those of PANI.[7]

TABLE II
The d-Spacing (D) and Crystallite Size (T) Corresponding to Different Crystalline peaks of PANI and SPANI

Sample	Crystallinity (%)	Crystalline peak 2θ (Degree)	Crystal plane (d_{hkl})	d-spacing (Å)	Crystallite size (Å)
PANI	37.3	6.3	–	14.01	58.4
		9.0	–	9.81	29.7
		14.8	d_{110}	5.98	28.2
		20.4	d_{-211}	4.35	17.9
		25.4	d_{211}	3.50	28.5
		33.6	d_{310}	2.66	9.7
SPANI	52.4	6.1	d_{010}	14.46	112.0
		9.7	d_{100}	9.10	346.4
		18.3	d_{-111}	4.84	78.8
		19.5	d_{200}	4.54	129.9
		20.2	d_{0-41}	4.39	152.1
		21.0	d_{011}	4.22	110.6
		24.0	d_{-2-21}	3.70	108.2
		24.9	d_{040}	3.57	36.4
		25.9	d_{3-40}	3.43	75.4
		27.1	d_{0-32}	3.28	99.6

The crystallinity of PANI and SPANI are 37.3 and 52.4%, respectively (Table II). Higher the degree of regularity in arrangement and ordering of the polymer chains higher is the crystallinity. This again depends on the type of interaction among the polymer chains; for example, an inter-chain hydrogen bonding or an electrostatic interaction among adjacent polymer chains. The higher crystallinity in SPANI indicates that the polymer chains in this polymer are more ordered compared to those of PANI. This may be due to the presence of strong inter-chain hydrogen bonding as well as to electrostatic (dipole–dipole) interactions involving both the amine and sulfonic acid groups present on this polymer chains. The calculated values of the d-spacing and crystallite size corresponding to the different crystalline peaks of PANI and SPANI are presented in Table II. As the crystal planes are different for PANI and SPANI, so their d-spacings cannot be compared. However, the overall d-spacing values for SPANI are higher than those of PANI. This may be due to the presence of the sulfonic group between the polymer chains, keeping the polymer backbones apart. The crystallite sizes are higher for SPANI compared to PANI. This result is also in agreement with the higher degree of crystallinity in SPANI compared to PANI. The conductivity of PANI is enhanced with the increase in crystallinity and/or decrease in d-spacings.[4,23,24] After sulfonation, both the degree of crystallinity and d-spacings are increased in SPANI. These two factors have opposite effect toward the modification of conductivity of SPANI and the effects are expected to be countervailed.

The crystal symmetry, space group unit cell dimension, and refinement parameters for PANI and SPANI are presented in Table III. Both the PANI and SPANI have triclinic crystal symmetry and a "P-1" space group. The space group may be described as a set of symmetry elements, and it is made up of two parts; a pattern unit and a repeat mechanism. The symbol P represents a primitive unit cell and −1 represents point groups.[15] After sulfonation, the dimension of the unit cell changes. The unit cell volume was found to increase after sulfonation. The definition of different parameters is as follows:

$$R_p = 100 \frac{\sum |y_i - y_{ci}|}{\sum y_i} \tag{4}$$

Here, R_p is the profile factor, y_i is the observed intensity, and y_{ci} is the calculated intensity at the ith step.

TABLE III
Crystal Data and Refinement Factors of PANI and SPANI Obtained After Running the DICVOL Program and Routine Profile Matching

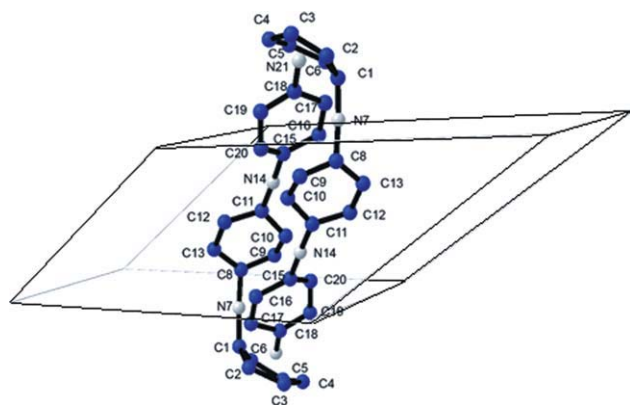| Parameters	PANI	SPANI
Crystal symmetry	Triclinic	Triclinic
Space group	P-1	P-1
a (Å)	8.6764	11.0075
b (Å)	17.3845	19.6161
c (Å)	13.6500	6.6314
α (deg)	25.884	118.726
β (deg)	109.084	96.623
γ (deg)	103.697	115.547
V (Å³)	840.83	1034.45
R_p	5.88	21.1
R_{wp}	12.7	28.6
R_{exp}	7.27	9.11
R_B	0.576	0.701
R_F	0.671	1.05
χ^2	3.05	9.89
d	0.3648	0.3168
Q_D	1.8049	1.8149
S	1.7	3.1

Figure 6 Arrangement of PANI chains in unit cell (resolved using the FOX v. 1.7. OSVN software after substituting the values of the unit cell dimensions and the space group obtained from the DICVOL program. The orientation was optimized and the configuration was randomized). Different bond length and bond angle values are presented in Table IV. [Color figure can be viewed in the online issue, which is available at www.interscience.wiley.com.]

$$R_{wp} = 100 \left[\frac{\sum w_i |y_i - y_{ci}|^2}{\sum w_i y_i^2} \right]^{1/2} \qquad (5)$$

Here, R_{wp} is the weighted profile factor, $w_i = 1/\sigma_i^2$, and σ_i^2 is the variance of the observation,

$$R_{exp} = 100 \left[\frac{(n-p)}{\sum w_i y_i^2} \right]^{1/2} \qquad (6)$$

Here, R_{exp} is the expected weighted profile factor, and n and p are the number of profile points and refined parameters, respectively.

$$R_B = 100 \frac{\sum |I_{obs} - I_{calc}|}{\sum |I_{obs}|} \qquad (7)$$

Here, R_B is the Bragg factor, I_{obs} is the observed integrated intensity, and I_{calc} is the calculated integrated intensity.

$$R_F = 100 \frac{\sum |F_{obs} - F_{calc}|}{\sum |F_{obs}|} \qquad (8)$$

Here, R_F is the crystallographic R_F factor, and F_{obs} is the observed structure factor
$F_{obs} = \sqrt{(I_{obs}/L)}$, where L is the Lorentz polarization factor.

$$\chi^2 = \sum w_i (y_i - y_{ci})^2 \qquad (9)$$

$$d = \sum \frac{[w_i(y_i - y_{ci}) - w_{i-1}(y_{i-1} - y_{ci-1})]^2}{\sum [w_i(y_i - y_{ci})]^2} \qquad (10)$$

Here, d is the Durbin–Watson statistic.

$$Q_D = 2 \left[\frac{(n-1)}{(n-p) - \frac{3.0901}{\sqrt{n+2}}} \right] \qquad (11)$$

Here, Q_D is the expected Durbin-Watson statistic.

$$S = \frac{R_{wp}}{R_{exp}} \qquad (12)$$

Here, S is the goodness of fit.

The refining of a crystal structure by minimizing the weighted squared difference between the observed and calculated patterns is carried out by the Rietveld method. The R factors, for example R_p and R_{wp}, are generally determined to realize the quality of the agreement between the observed and calculated profiles. These R factors are not satisfactory from a statistical point of view. Hence, statistically more significant parameters such as d, Q_D, and S are also calculated by FullProf. The relation $d < Q_D$ indicates a positive serial correlation, where successive values of the residuals tend to have the same sign. In profile refinement, this is the most common situation. The relation $Q_D < d < 4 - Q_D$ indicates that there is no correlation. When $d > 4 - Q_D$, there is a negative serial correlation: successive values of the residuals tend to have opposite signs.[32] For both PANI and SPANI, $d < Q_D$; this implies that there is a positive serial correlation between observed and calculated profiles. The closer the value of goodness of fit (S) to 1, the better is the agreement between observed and calculated profiles. The S value obtained for PANI and SPANI are 1.7 and 3.1, respectively. Therefore, the goodness of fit for PANI is superior to that of SPANI.

The arrangement of the PANI chains in the unit cell is shown in Figure 6 and different bond length and bond angle values are presented in Table IV (atom type and number are shown in the figure). Similar parameters for SPANI are shown in Figure 7 and Table V. In the case of PANI, the benzene rings and main chain nitrogen atoms present along the direction of the crystal planes (Fig. 6). Although the main chain amine nitrogens are on the same side, the nitrogens of adjacent polymer chains are apart from each other. Therefore, the probability for interchain H-bonding between amine nitrogen of one polymer chain with amine hydrogen of the other polymer chain adjacent to it is extremely low. All the benzene rings are not on the same plane, and some of the benzene rings have created a disordered region. In the case of SPANI, the benzene rings, main chain nitrogen atoms, and the sulfonic acid groups are arranged along the direction of the crystal planes and all atoms are on the same plane

TABLE IV
Different Bond Lengths and Bond Angles of PANI
(Atom Type and Number are Shown in Fig. 6)

Bond	Length (Å)	Angle	Value (°)
C1-C2	1.516962	C6-C1-C2	119.107325
C2-C3	1.489549	C1-C2-C3	118.357083
C3-C4	1.475690	C2-C3-C4	120.936627
C4-C5	1.511233	C3-C4-C5	118.926038
C5-C6	1.476291	C4-C5-C6	119.259761
C6-C1	1.473110	C5-C6-C1	118.496979
C1-N7	1.521246	C1-N7-C8	180.933210
N7-C8	1.529154	C13-C8-C9	118.326539
C8-C9	1.5215.8	C8-C9-C10	120.388901
C9-C10	1.518133	C9-C10-C11	118.965803
C10-C11	1.528447	C10-C11-C12	118.695451
C11-C12	1.525660	C11-C12-C13	118.821768
C12-C13	1.514192	C12-C13-C8	118.775460
C13-C8	1.518852	C11-N14-C15	181.248656
C11-N14	1.525787	C20-C15-C16	118.534982
N14-C15	1.523904	C15-C16-C17	120.254291
C15-C16	1.507508	C16-C17-C18	119.176829
C16-C17	1.487873	C17-C18-C19	118.752770
C17-C18	1.514903	C18-C19-C20	118.940873
C18-C19	1.517684	C19-C20-C15	120.939851
C19-C20	1.490466		
C18-N21	1.505829		
C20-C15	1.476943		

(Fig. 7). Sulfonic acid groups of two adjacent polymer chains are on the same side and close to each other, indicating the probability of some electrostatic interaction and intra-chain H-bonding between amine groups and sulfonic acid groups of the same polymer chain forming a six-member ring structure as well as inter-chain H-bonding between sulfonic acid groups of adjacent polymer chains. The degree of crystallinity is in good agreement with the arrangement of the polymer chains in the unit cell.

Scanning electron microscopy

The SEM images of PANI and SPANI are displayed in Figure 8. The PANI particles have a rod-like shape with a diameter of 0.5–0.7 µm and a length of 1.0–3.0 µm [Fig. 8(a)]. The shape of SPANI resembles a flat plate with a width of 0.4–1.6 µm and a length of 0.7–2.0 µm [Fig. 8(b)]. After sulfonation of PANI, its morphology is totally changed. Relatively well-defined crystals of SPANI are detectable from the SEM image, whereas those of PANI are not so clearly observed. These images are in sound agreement with their degree of crystallinity and crystallite size.

CONCLUSIONS

Sulfonated polyaniline (SPANI, 93–94% sulfonation) was found to be soluble in water (1.25 g/L at room

temperature). The hydrophilicity of PANI was increased significantly after sulfonation. The energies required for the π–π* and bipolaron/polaron transitions and the intensity of these transitions were decreased after sulfonation of PANI. The decrease in energies for the π–π* and bipolaron/polaron transitions is due to the extra protonation and to the formation of self-doped six-membered stable ring structure by the sulfonic acid group. The decrease in the intensity of these transitions is due to the decrease in electron density at the polymer backbone of SPANI because of the –R effect of the sulfonic acid
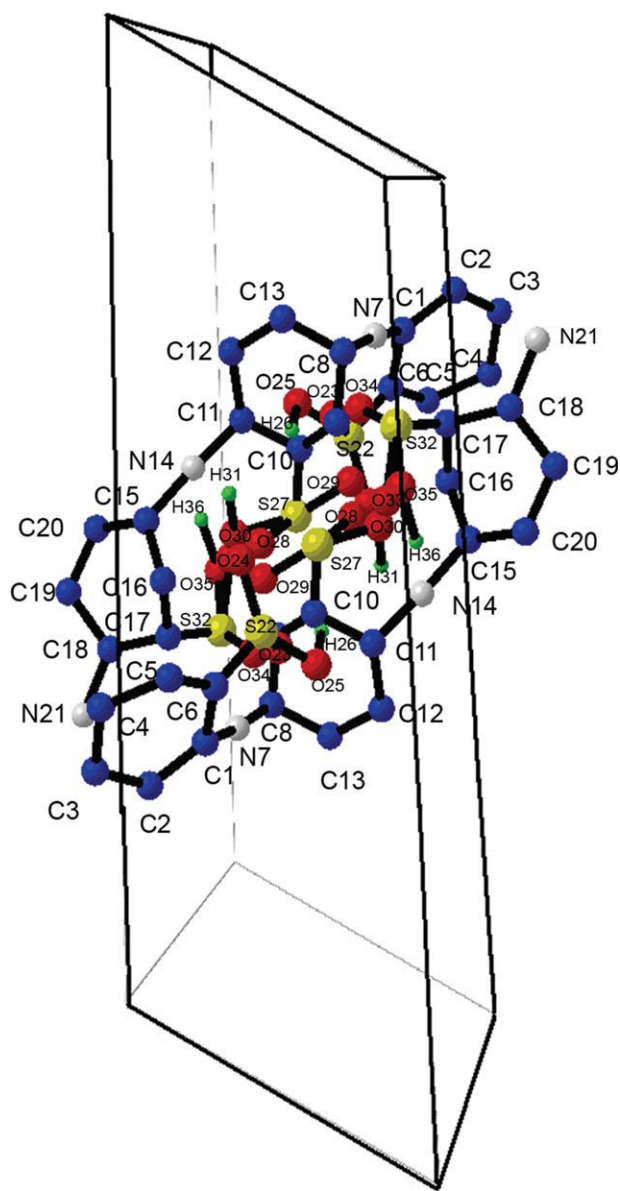

Figure 7 Arrangement of SPANI chains in unit cell (resolved using same method as PANI). Different bond length and bond angle values are presented in Table V. [Color figure can be viewed in the online issue, which is available at www.interscience.wiley.com.]

group. The lower conductivity of SPANI than that of PANI may be due to the –R effect of the sulfonic acid group and to the formation of more bipolarons through extra protonation. SPANI showed a more regular or ordered structure with a higher degree of crystallinity and greater crystallite sizes compared to PANI. After sulfonation the unit cell dimension and molecular arrangement in the unit cell of PANI were changed. The unit cell volume after sulfonation was found to increase. The positive serial correlation between observed and calculated profiles for all these polymers was observed and the goodness of fit for PANI and SPANI was found to be 1.7 and 3.1, respectively. After sulfonation, the morphology of PANI was changed from a rod-like shape to a flat-plate shape. SPANI appeared as sharper and well-defined crystals compared to PANI.

TABLE V
Different Bond Lengths and Bond Angles of SPANI
(Atom Type and Number are Shown in Fig. 7)

| Bond	Length (Å)	Angle	Value (°)
C1-C2	1.453593	C6-C1-C2	120.842931
C2-C3	1.522473	C1-C2-C3	119.222933
C3-C4	1.543159	C2-C3-C4	118.921571
C4-C5	1.521269	C3-C4-C5	117.036903
C5-C6	1.473950	C4-C5-C6	116.868648
C6-C1	1.510891	C5-C6-C1	120.561295
C1-N7	1.447998	C1-N7-C8	170.217549
N7-C8	1.446702	C13-C8-C9	111.625215
C8-C9	1.429008	C8-C9-C10	111.784993
C9-C10	1.496918	C9-C10-C11	113.956003
C10-C11	1.402449	C10-C11-C12	117.298582
C11-C12	1.555928	C11-C12-C13	119.338855
C12-C13	1.466783	C12-C13-C8	115.245235
C13-C8	1.456152	C11-N14-C15	175.068035
C11-N14	1.461525	C20-C15-C16	115.263896
N14-C15	1.511626	C15-C16-C17	112.454113
C15-C16	1.476623	C16-C17-C18	110.515985
C16-C17	1.429668	C17-C18-C19	116.251008
C17-C18	1.482845	C18-C19-C20	116.120333
C18-C19	1.510390	C19-C20-C15	115.731804
C19-C20	1.454543	C6-S22-O23	105.403397
C18-N21	1.483455	O23-S22-O24	109.067404
C20-C15	1.458133	O24-S22-O25	133.061716
C6-S22	1.491302	C6-S22-O25	108.191788
S22-O23	1.518557	S22-O25-H26	104.185670
S22-O24	1.481839	C10-S27-O28	106.910772
S22-O25	1.458773	O28-S27-O29	108.618996
O25-H26	1.508895	O29-S27-O30	135.688757
C10-S27	1.411338	C10-S27-O30	104.409974
S27-O28	1.449219	S27-O30-H31	101.012248
S27-O29	1.484064	C17-S32-O33	102.443073
S27-O30	1.472924	O33-S32-O34	105.044910
O30-H31	1.521069	O34-S32-O35	134.437657
C17-S32	1.445811	C17-S32-O35	110.836055
S32-O33	1.518811	S32-O35-H36	104.349246
S32-O34	1.520682		
S32-O35	1.479599		
O35-H36	1.505088		
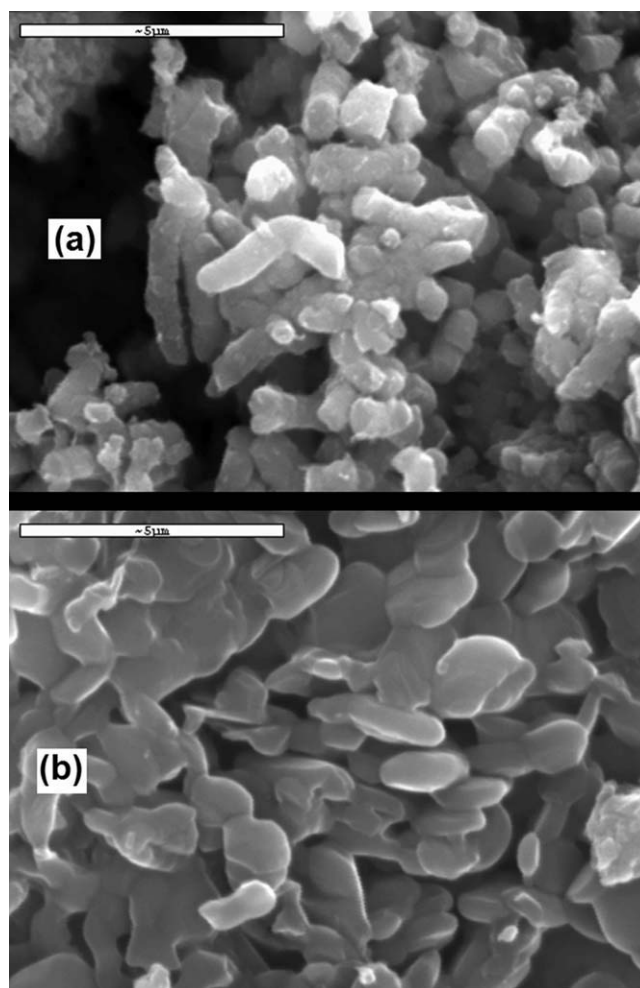
Figure 8 SEM images of (a) PANI and (b) SPANI (×10,000 magnifications, 20 kW, secondary electron imaging).

References

1. Angelopoulos, M. IBM J Res Dev 2001, 45, 57.
2. Gospodinova, N.; Terlemezyan, L. Prog Polym Sci 1998, 23, 1443.
3. Bhadra, S.; Singha, N. K.; Khastgir, D. Synth Met 2006, 156, 1148.
4. Bhadra, S.; Chattopadhyay, S.; Singha, N. K.; Khastgir, D. J Polym Sci Polym Phys 2007, 45, 2046.
5. Bhadra, S.; Khastgir, D. Polym Degrad Stab 2008, 93, 1094.
6. Bhadra, S.; Singha, N. K.; Khastgir, D. Eur Polym J 2008, 44, 1763.
7. Bhadra, S.; Khastgir, D. Polym Test 2008, 27, 851.
8. Iribarren, J. I.; Armelin, E.; Liesa, F.; Casanovas, J.; Aleman, C. Mater Corr 2006, 57, 683.
9. Wang, T.; Tan, Y. J. Corr Sci 2006, 48, 2274.
10. Wu, Q.; Qi, Z.; Wang, F. Synth Met 1999, 105, 191.
11. Wei, X. L.; Wang, Y. Z.; Long, S. M.; Bobeczko, C.; Epstein, A. J. J Am Chem Soc 1996, 118, 2545.
12. Tedesco, E.; Giron, D.; Pfeffer, S. Cryst Eng Comm 2002, 4, 393.
13. Nicolau, Y. F.; Djurado, D. Synth Met 1993, 55, 394.
14. Hageman, J. A.; Wehrens, R.; Gelder, R. D.; Buydens, L. M. C. J Comput Chem 2003, 24, 1043.
15. Ladd, M. F. C.; Palmer, R. A. In Structure Determination by X-Ray Crystallography; Plenum Press: New York, 1988; p 75.

16. Flandorfer, H.; Richter, K. W.; Giester, G.; Ipser, H. J Solid State Chem 2002, 164, 110.
17. Bubnova, R. S.; Krivovichevb, S. V.; Filatov, S. K.; Egorysheva, A. V.; Kargin, Y. F. J Solid State Chem 2007, 180, 596.
18. Sosnowska, I.; Przenioslo, R.; Schafer, W.; Kockelmann, W.; Hempelmann, R.; Wysocki, K. J Alloys Compd 2001, 328, 226.
19. Fernandez, S.; Mesa, J. L.; Pizarro, J. L.; Lezama, L.; Arriortua, M. I.; Rojo, T. Chem Mater 2002, 14, 2300.
20. Rodriguez-Carvajal, J.; Roisnel, T. Mater Sci Forum 2004, 443, 123.
21. Finar, I. L. In Organic Chemistry; 6th ed.; Addison Wesley Longman Limited: London, 1973; Vol. 1, p 33.
22. Li, Z. F.; Ruckenstein, E. J Colloid Interf Sci 2004, 269, 62.
23. Bhadra, S.; Singha, N. K.; Khastgir, D. J Appl Polym Sci 2007, 104, 1900.
24. Bhadra, S.; Singha, N. K.; Khastgir, D. Polym Int 2007, 56, 919.
25. Chiang, J. C.; Macdiarmid, A. G. Synth Met 1986, 13, 193.
26. Trchova, M.; Sedenkova, I.; Tobolkova, E.; Stejskal, J. Polym Degrad Stab 2004, 86, 179.
27. Bhadra, S.; Chattopadhyay, S.; Singha, N. K.; Khastgir, D. J Appl Polym Sci 2008, 108, 57.
28. Roisnel, J.; Rodriguez-Carvajal, J. In WINPLOTR, Laboratoire Leon Brillouin (CEA-CNRS) Centre d'Etudes de Saclay: Gif sur Yvette Cedex, France, 2000.
29. Boultif, A.; Louer, D. J Appl Cryst 2004, 37, 724.
30. Louer, D.; Louer, M. J Appl Cryst 1972, 5, 271.
31. Boultif, A.; Louer, D. J Appl Cryst 1991, 24, 987.
32. Rodriguez-Carvajal, J. In An Introducton to Program FullProf 2000. Version July 2001; Rodriguez-Carvajal, J. Ed.; Laboratoire Leon Brillouin: France, 2001.
33. Castellan, G. W. In Physical Chemistry; Narosa Publishing House: New Delhi, India, 1996; p 701.
34. Han, D.; Chu, Y.; Yang, L.; Liu, Y.; Lv, Z. Colloids Surf A 2005, 259, 179.
35. Kennedy, C. J.; Lerber, K. V.; Wess, T. J ePreserv Sci 2005, 2, 31.